Indian Journal of Pure & Applied Physics
Vol. 61, February 2023, pp. 124-131
DOI: 10.56042/ijpap.v61i2.69203

Physico-Chemical Study on Heat Transfer Property of Iron Oxide Nanofluid

Jayashree Sa & Ganeswar Nath*

Department of Physics, Veer Surendra Sai University of Technology, Burla Sambalpur, Odisha 768018, India

Received 28 November 2022; accepted 18 January 2023

The analytical characterization of thermophysical properties of metal oxide nanofluid has got significant attention in thermal industries due to their high capability of reducing energy loss and enhancing the efficiency of machinery parts. The fascinating heat transfer characteristics of green modulated iron oxide nanoparticles (IONPs) attain significant importance due to their wide range of diverse applications in different industries. In the current study, IONPs were successfully synthesized using an aqueous extract of Aloe vera (Aloe barbadensis) leaves to evaluate its effective thermophysical properties in base fluid like water. The average particle size of 11nm IONPs with its nanofluid of various volume concentrations 0.01 to 0.05 with a different temperature range of 30 °C to 50 °C shows an enhancement in thermal conductivity of 34.08% compared to distilled water (base fluid). Different characterization technique like Scanning electron microscopy (SEM), X-ray diffraction (XRD), Fourier transforms infrared (FTIR) spectroscopy, UV-visible spectroscopy, and particle size analyzer has been employed to get characteristic modification and formation of iron oxide nanoparticles. The experimentally measured values of thermal conductivity were compared with existing theoretical models for effective enhancement in thermophysical properties and the same was analyzed with the importance of green technique.

Keywords: Green synthesis; Iron oxide nanofluids; Thermal conductivity; Viscosity; Density

1 Introduction

Nanofluids are increasingly recognized as the upcoming generation of heat transfer fluids since they provide unique opportunities for enhancing thermal conductivity. They exhibit improved thermal performance as compared to conventional heat transfer fluids and fluids with tiny metallic particles[1]. As opposed to conventional particles, nanoparticles have a substantially higher relative surface area, which not only significantly enhances the ability to transport heat but also increases the stability of suspensions. Particles of the nanometer range, also known as nanoparticles, are distributed throughout liquids that are considered to be nanofluids[2]. Typically, these nanoparticles consist of metallic elements, oxides, graphite, carbides, Graphene, and carbon nanotubes among other materials. To dissolve the nanoparticles, base fluids such as distilled water, oil, glycerol, and ethylene glycol (EG) are utilized. Nanofluids exhibit superior convective heat transfer coefficients, thermal conductivity, and heat capacity, according to research findings[3,4]. The creation of stable and homogenized suspensions has been one of the topics of nanofluid research. Depending on specific factors, the preparation of nanofluids, particularly when using the two-step approach, is frequently accompanied by varying degrees of agglomerations.

The physical composition of the nanoparticle, the predominant particle charge, and the effectiveness of the van der Waals forces of attraction and repulsiveness are some of these factors[5]. Ultrasonic vibration is the most widely used deagglomeration technique for obtaining uniform dispersion[6]. In a two-step process for making nanofluid, first, the nanoparticles had to be made, and then they had to be thoroughly disseminated in the base fluid using an ultrasonic approach. Nanoparticles can be created using a variety of techniques. In contrast, "green" synthesis has drawn a lot of attention in the field of materials science as a cost-effective, long-term stable, and environmentally safe method for creating a variety of nanomaterials. Green synthesis is therefore seen as an essential tool to reduce the negative effects associated with the traditional methods of synthesis for nanoparticles, which are frequently utilized in laboratories and industry[7]. The process of creating nanoparticles utilizing natural extracts (from plants, microbes, *etc*.) is generally referred to as green, eco-friendly, biosynthesis of nanoparticles. By creating ecologically friendly nanoproducts, this method uses the concepts of green chemistry as a guide to

*Corresponding author: (E-mail: ganeswar.nath@gmail.com)

improving sustainability. By employing green technology, dangerous and expensive chemicals are avoided. The varieties of green-produced nanoparticles that are microscopically dispersed in the base conventional fluids determine the green/bio/eco-friendly nanofluids. In comparison to traditional nanofluids, green nanofluids are superior and offer numerous benefits. With safe handling provisions, it is possible to generate a wider range of green nanofluids that exhibit exceptional stability and favourable thermophysical characteristic. As an alternative working fluid, highly colloidal stable green nanofluids are therefore crucial for their efficient usage in various thermal systems. However, the study on environmentally friendly nanofluids that have been published over the last ten years in Science Direct[8].comshows that comparably less work has been done utilizing green nanofluids. Sundar et al. have investigated the thermal conductivity of nanofluids by chemically precipitating Fe_3O_4 nanoparticles and dispersing them in distilled water using a sonicator. They found that at 2.0 vol% nanofluid thermal conductivity enhancement was found to be 25% to 48% in the temperature range[9] of 20 °C to 60 °C.

In this work, we study how the temperature and nanoparticles' concentration affects the thermophysical properties of greenly synthesized water-based iron oxide nanofluid. Iron oxide nanoparticles can be produced utilizing plant resources, which are more environmentally friendly and compatible with a variety of applications because they don't require the use of hazardous chemicals. In this study, we have prepared iron oxide nanoparticles using aloe vera leaf extract. Aloe vera is chosen for the synthesis of iron oxide nanoparticles because it contains natural phytochemicals such as acemannan, aloin, aloe emodin, and aloesin, which act as natural capping and reducing agents[10].

2 Materials and Methods

2.1 Materials

Anhydrous $FeCl_3$ was purchased from NICE Chemicals (P) Ltd., Kerla, India. $FeSO_4.7H_2O$ and NaOH were purchased from Isochem laboratory, Kerla, India. Distilled water was used to prepare all the aqueous solutions.

2.2 Preparation of Fe_3O_4 nanoparticles

2.2.1 Preparation of Leaf Extract

Fresh aloe vera leaves were collected from the local garden. The leaves were carefully cleansed with purified water. Almost 25 grams of fresh aloe vera leaves were cut into small pieces and dissolved in 150 mL of distilled water, then stirred at 50 °C for 1 hr with a magnetic stirrer. After cooling, the mixture was filtered using Whatman filter paper. Finally, the extract was stored at 5-10 degrees Celsius and can be utilized as a reducing and stabilizing agent.

2.2.2 Synthesis of Iron Oxide Nanoparticles using Aloe Vera Leaf Extract

Anhydrous $FeCl_3$ and $FeSO_4.7H_2O$ were used as precursors to make iron oxide nanoparticles. To synthesize Fe_3O_4-NPs, a yellowish colloidal solution was made by mixing a 100mL solution of Fe^{3+} and Fe^{2+} in a 2:1 M ratio with 50mL of aloe vera extract in a 2:1 ratio. Then, under constant stirring, the freshly made 1M of NaOH was added drop-by-drop to the solution. The solution's pH level was raised to 11. The solution was then agitated for 1 hour to homogenize it and ensure that the reaction was completed. The development of iron oxide nanoparticles is indicated by a shift in the colour of the solution from yellowish brown to dark black. A permanent magnet was then used to separate the as-synthesized Fe_3O_4-NPs. The Fe_3O_4-NPs were centrifuged at 3500rpm and deionized water was used to wash them numerous times. For 24 hours, the nanoparticles were dried at 70 °C in an oven. For further characterization, the dried material was kept in an airtight container. Fig. 1 describes the methodical procedures for preparing nanoparticles. The chemical reaction for the formation of Fe_3O_4-NPs is given below.

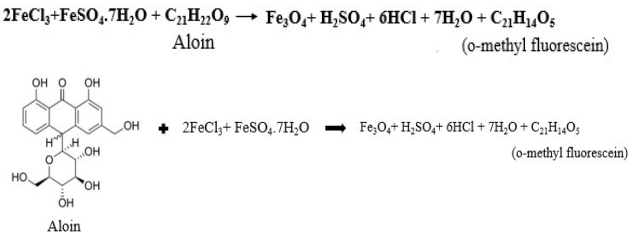

2.2.3 Preparation of Iron Oxide Nanofluid

As the base fluid, distilled water was used to prepare iron oxide nanofluid. Here, we've utilized a bath sonicator and a mechanical stirrer and prepared five different concentrations of nanofluid, namely 0.01, 0.02, 0.03, and 0.04, 0.05 vol%. Initially, in a beaker with 100 mL of distilled water, 51.8 mg of iron oxide nanopowder was weighed and added to prepare 0.01 vol%. The solution was subjected to a bath Sonicator for 60 minutes. High-frequency sound waves produced by the sonication effect allow for the

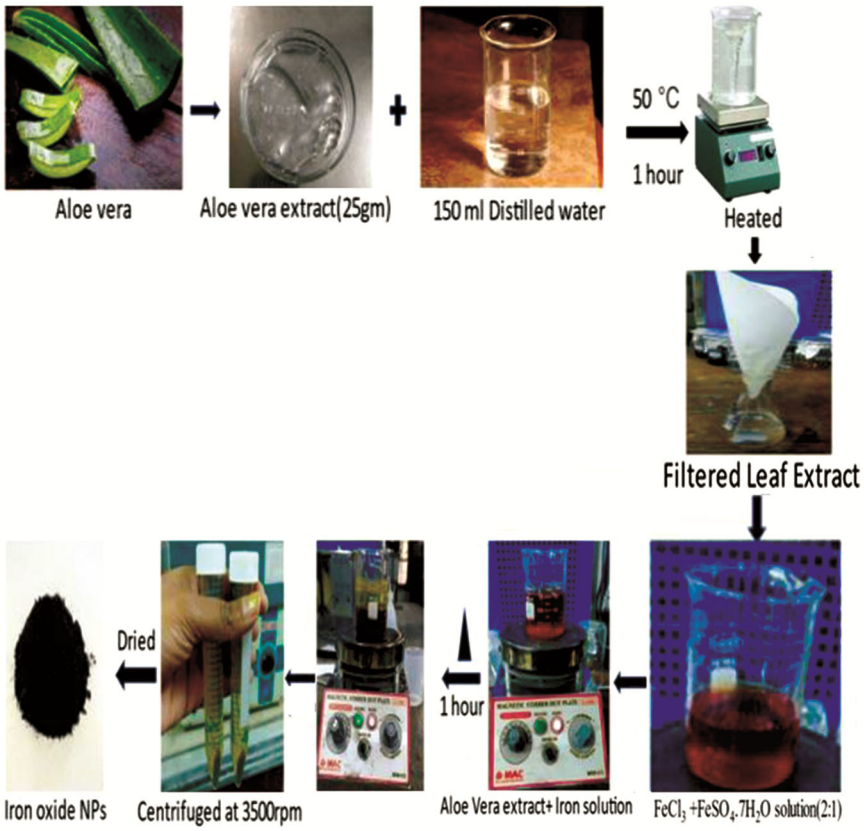

Fig. 1 — Preparation of nanoparticles from fresh aloe vera leaves by green synthesis method.

well-diffusion of nanoparticles into the base fluid. After sonication the solution was agitated with a mechanical stirrer for about 30 minutes, then cooled and placed in a moisture-free airtight container for storage. The procedure was repeated for other concentrations. With the help of sonication and stirring, allow the nanoparticles to disperse effectively in the distilled water to avoid the agglomeration of nanofluid. Eq.1 can be used to estimate the volume concentration of the nanofluid[11].

$$\text{Volume fraction, } \Phi = \frac{\frac{W_{np}}{\rho_{np}}}{\frac{W_{np}}{\rho_{np}} + \frac{W_{bf}}{\rho_{bf}}} \quad \ldots (1)$$

Where, W_{np} = weight of iron oxide nanoparticle, ρ_{np} = density of iron oxide nanoparticles, W_{bf} = weight of distilled water (base fluid), ρ_{bf} = density of distilled water (base fluid). Fig. 2 details the methodical procedures for preparing nanofluid.

2.2.4 Experimental Measurement of Nanofluid

The water-based iron oxide nanofluid's thermal conductivity was measured by a TEMPOS thermal analyzer using a KS-3 sensor (length of 60mm and diameter of 1.3mm) that operates in a low-power mode with ±10% accuracy which is specially designed for liquid samples. To determine the iron oxide nanofluid's thermal conductivity at various temperatures, the sample bottle is set up in a calorimeter setup with the sensor KS-3 inserted perpendicularly into it at various temperatures for different vol%. For greater precision at each temperature, each sample's thermal conductivity was tested three times. Equation (2) was used to determine the enhancement in thermal conductivity of iron oxide nanofluid[12].

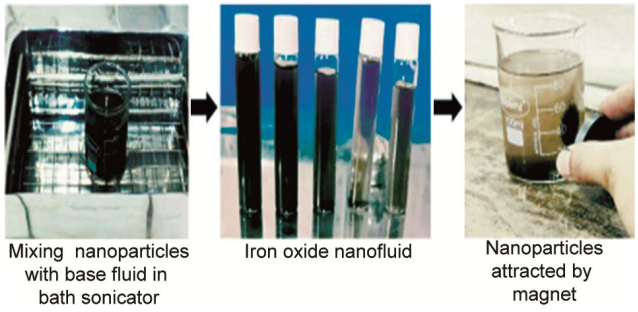

Fig. 2 — Preparation of iron oxide nanofluid.

$$\%K_{Enha} = \frac{K_{nf} - K_{bf}}{K_{bf}} \times 100 \quad \text{... (2)}$$

Where the thermal conductivity of iron oxide nanofluid and base fluid is denoted by K_{nf} andK_{bf}respectively[12].

The mass balance formula[13] was used to determine density the of iron oxide nanofluid which is given by Eq. (3)

$$\rho_{nf} = \phi\rho_{np} + (1-\phi)\rho_{bf} \quad \text{... (3)}$$

Where, the density of iron oxide nanofluid, nanoparticles, and distilled water (base fluid) are represented by ρ_{nf}, ρ_{np}, and ρ_{bf} respectively.ϕ is the nanofluid's volume concentration. The kinematic viscosity of iron oxide nanofluid at various temperatures was measured by a Redwood viscometer.

2.2.5 Theoretical Models

The Maxwell model[14] is an eminent approach to determining the thermal conductivity of a nanofluid. This model is appropriate for evenly sized, non-interacting, randomly dispersed homogeneous nanofluids with low volume concentration. Eq. (4) gives the Maxwell model's estimate of a nanofluid's thermal conductivity.

$$K_{nf} = \frac{K_{np} + 2K_{bf} + 2\phi(K_{np} - K_{bf})}{K_{np} + 2K_{bf} - \phi(K_{np} - K_{bf})} K_{bf} \quad \text{... (4)}$$

The thermal conductivity of a nanofluid is determined by Eq. (5) in accordance with the Hamilton-Crosser model[15].

$$K_{nf} = \frac{K_{np} + (n-1)K_{bf} - (n-1)(K_{bf} - K_{np})\phi}{K_{np} + (n-1)K_{bf} + (K_{bf} - K_{np})\phi} K_{bf} \quad \text{... (5)}$$

Where the empirical shape factor and sphericity[15]of the particle are denoted by n and ψ respectively. For spherical particles,n = 3/ψ, with ψ= 1.

When $K_{np} >> K_{bf}$, $K_{nf} = K_{bf}\left(\frac{1+2\phi}{1-\phi}\right)$

3 Characterization

BRUKER D8 ADVANCE diffractometer was used to determine the crystal structure of iron oxide nanoparticles. The diffractograms were produced using a 2θ variation between 10° and 80° operated at 30mA and 40kV. Iron oxide nanoparticles' peak pattern and crystalline structure have been examined by PANalytical X'Pert Highscore software. SEM (HITACHI-SU 3500) was used to evaluate the morphological behaviour change of iron oxide nanoparticles. FTIR Spectrophotometer (Bruker alpha-II USA) was used to analyze the functional group present in iron oxide nanofluid, which was operated in the transmittance mode and the wavenumber range of 500-4000cm^{-1}. The UV-Visible spectrophotometer (UV-19001) was used at room temperature to capture the absorption spectra of iron oxide nanoparticles[12].

4 Results and Discussion

4.1 XRD Analysis

Utilizing XRD data analysis on green-produced iron oxide nanoparticles, the formation of the nanocrystalline phase was verified. With increasing X-ray beam intensity, the diffractograms peak pattern at 30.10°, 35.40°, 43.09°, 53.51°, 56.98°, 62.65°, and 74.10° with miller indices (2 2 0), (3 1 1), (4 0 0), (4 2 2), (5 1 1), (4 4 0), (5 3 3) respectively confirm the presence of iron oxide according to JCPDS file no:01-089-6466 as shown in Fig. 3. Iron oxide traces have an orthorhombic structure, which is supported by the lattice space group-57 having cell parameters a = 2.7992, b = 9.4097, and c = 9.4832. The particle size or grain size of iron oxide was determined using the Debye-Scherer formula[12] to confirm its nanoscale size.

$$D_{hkl} = \frac{k\lambda}{\beta_{hkl}\cos\theta_{hkl}} \quad \text{... (6)}$$

Where $\beta_{hkl}$is the full width half maximum intensity, θ_{hkl} is the Bragg's angle, D_{hkl} is the average crystallite size, k (=0.9) is the Scherer's constant and λ

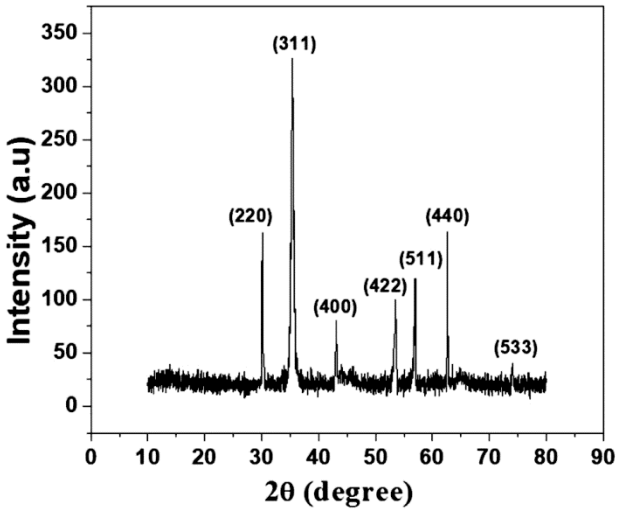

Fig. 3 — X-ray diffraction spectra of synthesized iron oxide nanoparticle.

(=0.154nm) is the X-ray wavelength. It was determined that the average crystalline size was 11 nm.

4.2 SEM Analysis

The SEM revealed that the particles appeared to be smoothly sphere-shaped as shown in Fig. 4. Particle diameter measurements following ultrasonication dispersion revealed a normal distribution curve with an axis of 35 nm. More than 95% of the nanoparticles had sizes under 50 nm.

4.3 FTIR Spectroscopy Analysis

Fourier transform infrared spectroscopy confirms the iron oxide nanofluid synthesis. Infrared radiation was allowed to interact with the iron oxide molecules in the nanofluid. At some quantized frequencies, various bending and stretching vibrations occur. Absorption takes place when the infrared waves are coupled with the vibration of iron oxide molecules. This absorption excites the iron oxide nanoparticles into various excited vibrational states. Through the analyzer, absorption spectra with respect to the wavelength in the range of 400 nm to 4000 nm were obtained. The stretching and bending bonds of the unknown molecules can be compared with the predefined values for various bonds of known molecules. Fig. 5 shows the absorption spectra of the prepared sample. The presence of the O-H group is indicated by the occurrence of a peak at 3314 cm^{-1}. At 1641 cm^{-1}, the carbonyl group's stretching vibration is seen[16]. C-O bonds are responsible for the peak at about 1054 cm^{-1}. Aliphatic C-H peaks first appeared at 2978 cm^{-1}. The appearance of these peaks indicates that organic molecules have functionalized NPs. The impact of aqueous leaf extract on IONPs led to coating development and herbal biochemical compound stabilization. Nanostructures having hydrophilic groups like hydroxyl, carbonyl, and C-O become more functionalized as a result of interactions with water molecules. In between 400-700 cm^{-1} we have found inorganic lattice vibration. The Fe-O stretching is responsible for the presence of a new sharp peak at around 581 cm^{-1} in Fe3O4 NPs[17,18]. This indicates that magnetite particles were formed by using aloe vera leaf extract.

4.4 UV-Visible Spectroscopy Analysis

The spectroscopic investigations of the sample were carried out when it was exposed to UV light to determine the optical and structural characteristics of the iron oxide nanoparticles. Iron oxide nanoparticles' UV-vis spectrum was determined at room temperature and shown in Fig. 6. The production of iron

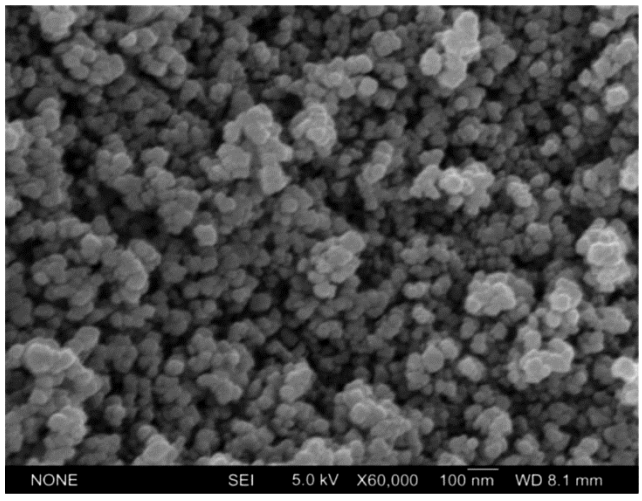

Fig. 4 — SEM image of synthesized iron oxide nanoparticle.

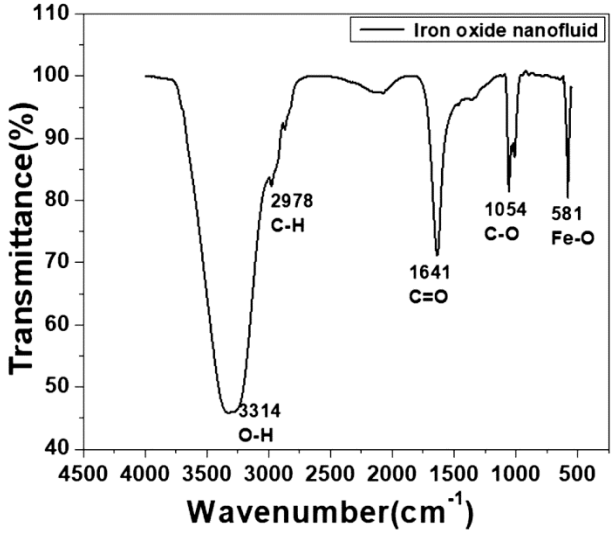

Fig. 5 — FTIR of iron oxide nanofluid.

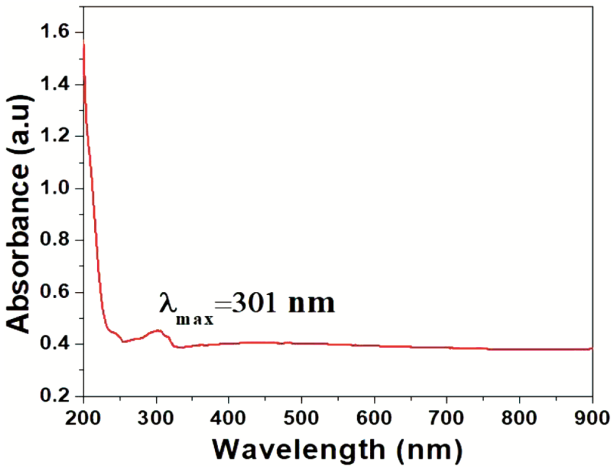

Fig. 6 — UV-Visible spectra of iron oxide nanofluid.

oxide nanoparticles is shown by the absorbance peak at 301 nm [19].

4.5 Particle Size Distribution Analysis

The Malvern Mastersizer -3000 operated with a high-intensity laser source and an ultrasonic cleaner was used to perform the particle size distribution of iron oxide nanofluid as illustrated in Fig. 7. The distribution of oxide nanoparticles is found to be more uniform with a narrow distribution range, with a particle size range of roughly 1 nm to 60 nm and a mean particle size of 22 nm.

4.6 Thermophysical Properties Analysis

The different thermophysical properties like density and kinematic viscosity of synthesized iron oxide nanofluids are measured for analysis and increment in thermal conductivity of nanofluid. The method of synthesis and characterization provides the indigenous and inherent thermal properties of nanomaterial and its nanofluid with supporting mechanisms. Nanoparticle concentration has a significant impact on different thermophysical properties like density, kinematic viscosity, and thermal conductivity. The density of nanofluid increases linearly as the particle volume concentration increases, as shown in Fig. 8. The ability of a nanofluid to absorb heat improves as the volume concentration of nanoparticles grows, that is why the density of a nanofluid rises dramatically as the particle volume concentration rises[20].

The effective kinematic viscosity of iron oxide nanofluids was determined for various concentrations ranging from 0.01- 0.05 vol% with respect to a temperature range ranging from 30 °C - 50 °C, as shown in Fig. 9. The kinematic viscosity of 0.01 vol% iron oxide nanofluid decreases from 0.1041 mm2/s to 0.0777 mm2/s as the temperature rises from 30 °C to 50 °C. The results show that the kinematic viscosity of nanofluid decreases as temperature rises due to the weakening of intermolecular forces between nanoparticles. It should also be noted that as the nanoparticle concentration of iron oxide nanofluid increases, so does the kinematic viscosity of the iron oxide nanofluid. Increases in viscosity are caused by an increase in the concentration of Fe_3O_4 nanoparticles in the fluid, which increases friction and fluid flow resistance[21]. When particle concentration is increased from 0.01 to 0.05 vol% at 30 °C, the kinematic viscosity increases from 0.1041 mm2/s to 0.1256 mm2/s. This result matches the outcome of the experiment conducted by Gao *et al.*[22].

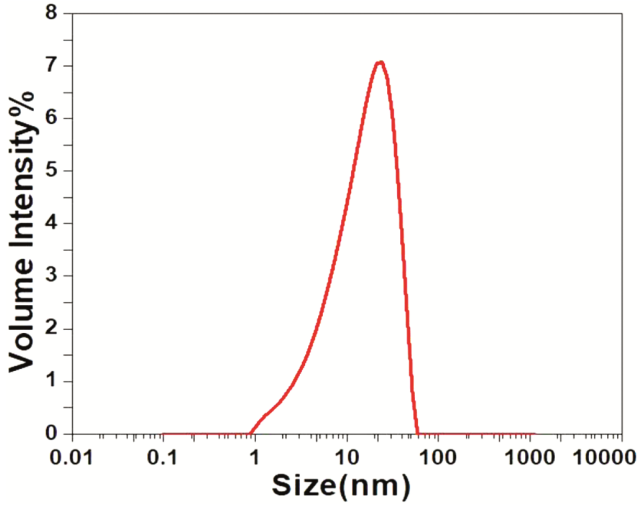

Fig. 7 — Particle size distribution of iron oxide nanofluid.

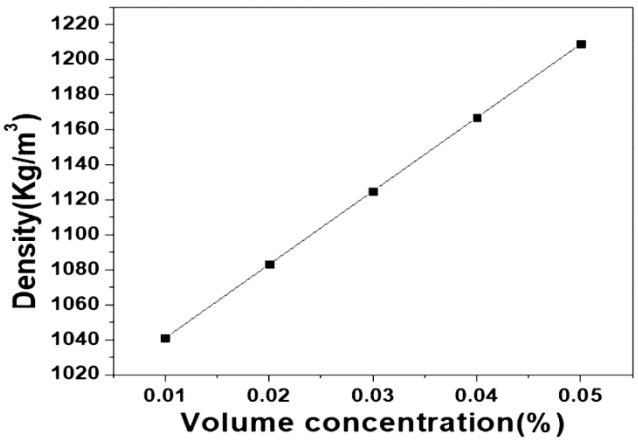

Fig. 8 — Density of iron oxide nanofluid.

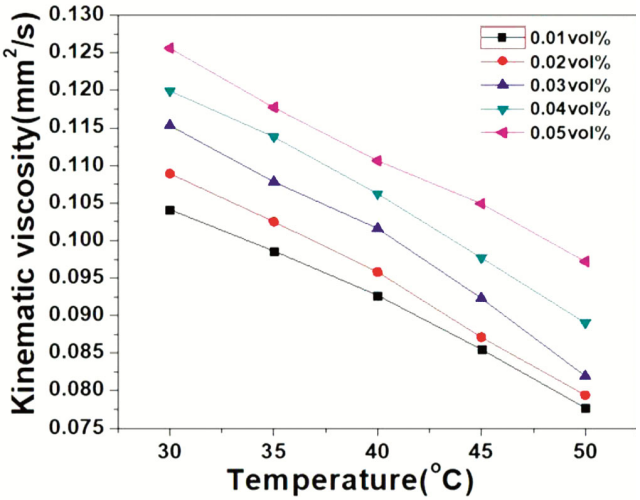

Fig. 9 — Kinematic viscosity of iron oxide nanofluid.

With the temperature rise, the iron oxide nanofluids'thermal conductivity also rises for various concentrations, as shown in Fig. 10 & 11 depicts the corresponding enhancement in thermal conductivity for each volume concentration at various temperatures. The graph shows that when the volume fraction is changed from 0.01 to 0.05, the thermal conductivity increases from 3.90% to 16.97% at 30 °C. When the temperature is raised from 30 °C to 50 °C, the thermal conductivity increases from 0.689 W/mK to 0.834 W/mK, with an enhancement from 16.97% to 34.08% for 0.05 vol%, which is shown to be higher in the current case than in the literature[23]. The nanofluids' thermal conductivity rises with temperature as Brownian motion and particle kinetic energy rise. Increased Brownian motion allows for more convection, causing the particle to collide with the base fluid more frequently, increasing heat transfer processes which result in increased thermal conductivity[24]. When the kinetic energy of particles increases, more particles collide, increasing heat transfer[25]. The base fluid's properties also influence how the nanofluids'thermal conductivity changes with temperature and concentration[26–28]. Thermal conductivity is continuously rising in the green synthesis process since distilled water is used as the base fluid. This is because water molecules have a lot of H-bonds, which can store energy instead of transfer it [29]. Fig. 12 depicts a comparison of the thermal conductivity of Fe_3O_4 nanofluid with a theoretical model. According to the Hamilton-crosser and Maxwell models, the thermal conductivity of iron oxide nanofluid increases from 0.606 to 0.64 W/mK and 0.605 to 0.638 W/mK, respectively, whereas the experimentally calculated thermal conductivity rises from 0.612 to 0.703 W/mK when temperature increases from 30 °C to 50 °C for 0.01 vol% nanofluid. The elegance of the increase in thermal conductivity can be attributed to the green nanoparticle preparation methods, in which aloe vera leaf extract contains a variety of phytochemical compounds that function as both reducing and capping agents for keeping the nanoparticles in a base fluid that supports micro convention[30]. Various controlling factors, such as the type of phytochemicals, particle concentration,

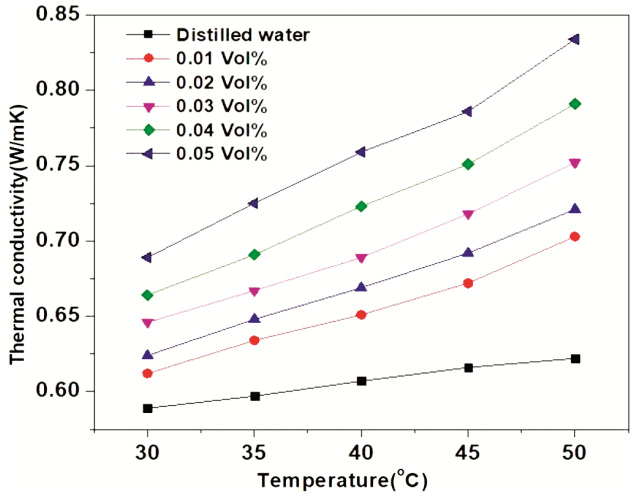

Fig. 10 — Variation of thermal conductivity of iron oxide nanofluid with temperature.

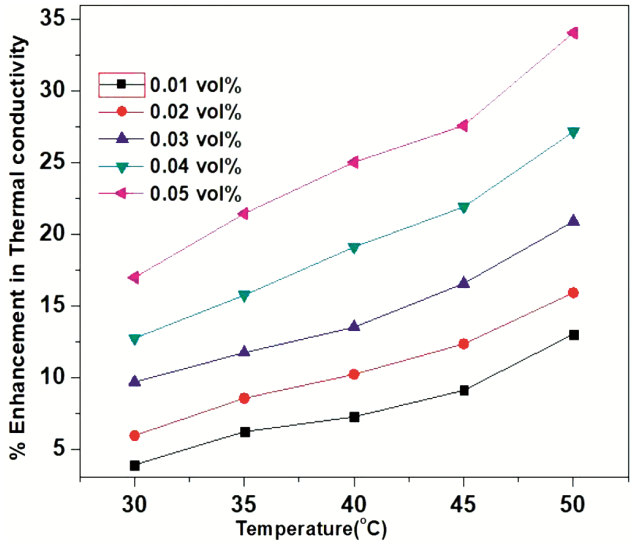

Fig. 11 — Variation of percentage increment in thermal conductivity of iron oxide nanofluid with temperature.

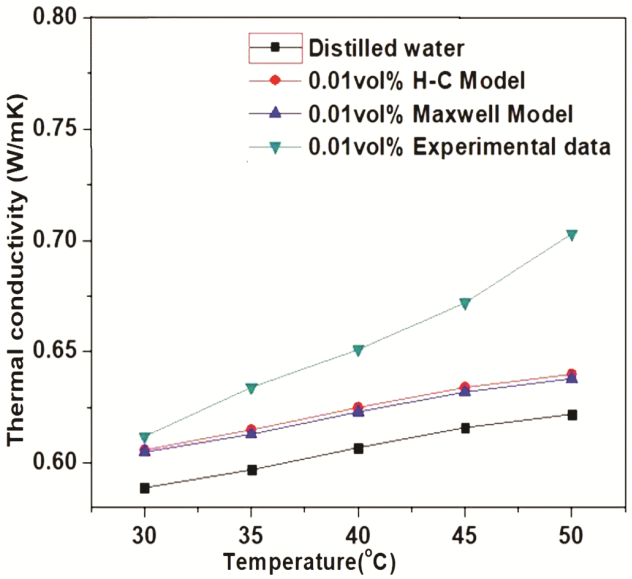

Fig. 12 — Comparison of thermal conductivity of iron oxide nanofluid with theoretical models.

and pH keep the yield and stability of the nanofluid within the base fluid while increasing the thermal conductivity[31]. Additionally, this rise in thermal conductivity is supported by the presence of a greater interfacial area[30] between distilled water and iron oxide nanoparticles as a result of a reduction in the intermolecular distance between the nanoparticles [32-34].

5 Conclusions

Using aloe vera leaf extract and the green synthesis technique, iron oxide nanoparticles were prepared successfully. By using these nanoparticles, nanofluids of various volume % were prepared by the ultrasonic method, which had the advantages of low agglomeration, high stability, and dispersion. The production of iron oxide nanoparticles with a size of 11 nm is confirmed by the orthorhombic crystal structure and high crystallinity index. The produced iron oxide nanoparticle's spherical shape is confirmed by the morphological study at various magnifications. The FTIR spectra show the various functional groups with a distinct peak for iron oxide nanoparticles present at wave number 581cm^{-1}. The distribution of iron oxide nanoparticles is found to be more uniform with a narrow distribution range, with a particle size range of roughly 1 nm to 60 nm and a mean particle size of 22 nm. The density of iron oxide nanofluid increases as the particle concentration increases. The highest kinematic viscosity of nanofluid was 0.1256 mm^2/s at 30°C for a 0.05% volumetric concentration of iron oxide nanoparticles. Different characteristic evaluations of the nanoparticles corroborated the rise in thermal conductivity with volume concentration and temperature. Thus, it can be concluded that using green technologies to create nanoparticles has numerous advantages over traditional techniques of preparation, including an improvement in thermal conductivity of up to 34.08% at higher concentrations like 0.05 volume fraction of nanofluid.

Conflicts of interest

The authors declare no conflicts of interest.

Acknowledgment

The vice chancellor of VSSUT, Burla, is gratefully acknowledged by the authors for providing a variety of laboratory facilities for conducting the research.

References

1 Barai D P, Bhanvase B A & Saharan V K, *Ind Eng Chem Res,* 58 (2019) 8349.
2 Chougule S S & Sahu S K, *J Nanotechnol Eng Med,* 5 (2014) 010901.
3 Chaurasia P, Kumar A, Yadav A, Rai P K, Kumar V & Prasad L, *SN Appl Sci*, 1 (2019) 1.
4 Tembhare S P, Barai D P & Bhanvase B A, *Renew Sust Energ Rev,* 153 (2022) 111738.
5 Ajayi O O, Ukasoanya D E, Ogbonnaya M, Salawu E Y, Okokpujie I P, Akinlabi S A, Akinlabi E T & Owoeye F T, *Procedia Manuf,* 35 (2019) 112.
6 Sheikholeslami M, Rezaeianjouybari B, Darzi M, Shafee A, Li Z & Nguyen TK, *Int J Heat Mass Transf,* 141 (2019) 974.
7 Singh J, Dutta T & Kim K H, *J Nanobiotechnol*, 16 (2018) 1.
8 Kumar L H, Kazi S N, Masjuki H H & Zubir M N M, *Chem Eng J*, 429 (2022) 132321.
9 Sundar L S, Singh M K & Sousa A, *Int Commun Heat Mass Transf*, 44 (2013) 7.
10 Medda S, Hajra A & Dey U, *Appl Nanosci*, 5 (2015) 875.
11 Sa J & Nath G, *Adv Nat Sci: Nanosci Nanotechnol*, 13 (2022) 025011.
12 Sa J & Nath G, *Mater Today: Proc,* 62 (2022) 5877.
13 Yew Y P, Shameli K & Miyake M, *Nanoscale Res Lett*, 11 (2016) 1.
14 Maxwell J C, 2nd Edn, *A treatise on electricity and magnetism*, Clarendon Press, Oxford, 1881.
15 Hamilton R L & Crosser O K, *Ind Eng Chem*, 1 (1962) 187.
16 Mahdavi M, Namvar F, Ahmad M B & Mohamad R, *Molecules,* 18 (2013) 5954.
17 Demir A, Topkaya R & Baykal A, *Polyhedron*, 65 (2013) 282.
18 Basavegowda N, Magar K B S, Mishra K & Lee Y R, *New J Chem*, 38 (2014) 5415.
19 Niraimathee V A, Subha V & Ramaswami S E R, *Int J Env Sustain Dev*, 15 (2016) 1.
20 Hussein A M, Sharma K V, Bakar R A & Kadirgama K, *J Nanomater*, 2013 (2013) 1.
21 Sadri R, Ahmadi G, Togun H, Dahari M, Kazi S N, Sadeghinezhad E & Zubir N, *Nanoscale Res Lett*, 9 (2014) 1.
22 Gao D, Bai M, Hu C, Lv J, Wang C & Zhang X, *Nanotechnol*, 31 (2020) 495402.
23 Hemmat E M, Yan W M, Akbari M, Karimipour A & Hassani M, *Int Commun Heat Mass Transf,* 68 (2015) 248.
24 Chon C H, Kihm K D, Lee S P & Choi S U S, *Appl Phy Lett*, 87 (2005) 153107.
25 Nichols G, Byard S, Bloxham M J, Botterill J, Dawson N J, Dennis A, Diart V, North N C & Sherwood J D, *J Pharm Sci,* 91 (2002) 2103.
26 Teleki A, Wengeler R, Wengeler L, Nirschl H & Pratsinis S, *Powder Technol*, 181 (2008) 292.
27 Ghadimi A & Metselaar I H, *Exp Therm Fluid Sci*, 51 (2013) 1.
28 Barai D, Bhanvase B & Żyła G, *Nanomater*, 12 (2022) 1.
29 Sonawane S S, Khedkar R S & Wasewar K L, *J Exp Nanosci,* 10 (2015) 310.
30 Sa J & Nath G, *J Sci Ind Res,* 81 (2022) 671.
31 Malik P, Shankar R, Malik V, Sharma N & Mukherjee T K, *J Nanoparticles*, 2014 (2014) 1.
32 Dwivedi A D & Gopal K, *Colloids Surf A: Physicochem Eng Asp*, 369 (2010) 27.
33 Rostamian S H, Biglari M, Saedodin S & Esfe MH, *J Mol Liq*, C (2017) 364.
34 Xuan Y & Li Q, *Int J Heat Fluid Flow*, 21 (2000) 58.